JOURNAL OF ADVANCED DIELECTRICS
Vol. 5, No. 1 (2015) 1550005 (9 pages)

DOI: 10.1142/S2010135X15500058

World Scientific
www.worldscientific.com

Study on properties of tantalum-doped $La_2Ti_2O_7$ ferroelectric ceramics

Chunchun Li*,†,‡, Jibran Khaliq‡, Huanpo Ning‡, Xiaoyong Wei*,§, Haixue Yan‡ and Michael J. Reece‡

*Electronic Materials Research Laboratory
Key Laboratory of the Ministry of Education & International Center for Dielectric Research
Xi'an Jiaotong University, Xi'an 710049, P. R. China
and
†College of Information Science and Engineering
Guilin University of Technology, Guilin 541004, P. R. China
and
‡School of Engineering and Material Science
Queen Mary University of London, London E1 4NS, UK
§wdy@mail.xjtu.edu.cn

Received 23 January 2015; Revised 2 February 2015; Accepted 12 February 2015; Published 31 March 2015

A series of ceramics with a general formula, $La_2Ti_{2-x}Ta_xO_7$, in which $x = 0.05, 0.1, 0.2$, and 0.3, were prepared by Spark Plasma Sintering (SPS). Effects of tantalum substitution for titanium on the structure, dielectric, and piezoelectric properties were studied. Results revealed that the structure changed gradually from 4-layer to 3-layer due to the higher valence of Ta. The solid solution limit of tantalum in $La_2Ti_2O_7$ lattice was in the proximity of $x = 0.2$. The ferroelectric Curie temperature (T_c) decreased with increasing tantalum doping content. dc resistivity reached a maximum value at $x = 0.2$ with a value of $\sim 1.0 \times 10^8 \Omega \cdot$ cm at 600°C. The influence of texture on the piezoelectric properties of $La_2Ti_{2-x}Ta_xO_7$ ceramics was also investigated. A maximum d_{33} value ~2.1 pC/N was obtained at $x = 0.2$.

Keywords: Piezoelectric ceramics; Curie temperature; piezoelectric coefficient.

1. Introduction

With the recent progress and development in automotive, aerospace, and power generating industries, there has been an ever-increasing need for actuators and sensors that can be operated at high temperatures.[1–4] Piezoceramics are the best candidates in terms of sensitivity, cost, and design, compared with other different types of acoustic and strain sensors.[3] Commercially, the operating temperature of piezoelectric materials is limited to 1/2 T_c.[5] So the general need for stable piezoelectric materials over a wide temperature range evokes an increasing interest to develop piezoceramics with high T_c. Currently, dominating studies on high-temperature piezoelectric ceramics are focused on lead-free (K,Na)NbO_3-based ceramics[6,7] and bismuth layer-structured ferroelectric ceramics, such as $CaBi_2Nb_2O_9$, $Bi_4Ti_3O_{12}$, and $CaBi_4Ti_4O_{15}$ and their variants, etc.[3,8,9] However, the Curie points of these piezoelectric ceramics are limited to 950°C, limiting their practical applications at very high temperatures. The highest Curie temperatures have been found in some perovskite-like layer structured (PLS) ferroelectrics with a general formula of $A_2B_2O_7$, such as $La_2Ti_2O_7$($T_c \sim 1461$°C), $Nd_2Ti_2O_7$($T_c \sim 1482$°C), $Sr_2Nb_2O_7$ ($T_c \sim 1327$°C), etc.[10–17] Their super-high Curie points has stimulated considerable interests in this system.

Among them, $La_2Ti_2O_7$ is a promising candidate for high-temperature piezoelectric sensors due to its piezoelectric activity and extremely high Curie point. At room temperature, $La_2Ti_2O_7$ adopts primitive monoclinic structure with a polar space group of $P2_1$. The piezoelectric coefficient d_{33} of $La_2Ti_2O_7$ single crystal was reported as 16 pC/N.[17] However, polycrystalline ceramics are difficult to be poled because of the low crystal symmetry, which offers few equivalent directions to polarization, and the randomly oriented grains which make the E_c of ceramics much higher than those of single crystals.[10,12] Thus, the d_{33} of $La_2Ti_2O_7$ ceramics is much lower than that of the single crystal (in some cases, its d_{33} cannot be characterized). In recent years, there have been an effort to enhance the piezoelectric performance of $La_2Ti_2O_7$ ceramics via cations modification and certain special fabrication methods, for example, texturing technologies.[12,18] Yan *et al.*[12] fabricated high textured $La_2Ti_2O_7$ ceramics by spark plasma sintering (SPS) and they reported an improvement in piezoelectric coefficient d_{33} from ~1.6 pC/N to ~2.6 pC/N for textured ceramics synthesized from

nanosized $La_2Ti_2O_7$ powders. More recently, enhancement of piezoelectric coefficient of $La_2Ti_2O_7$ ceramics was achieved by Ce^{3+} substitution, and the highest value of $d_{33} \sim 3.9$ pC/N was obtained for 7.5 mol% on A-site.[18]

In lead zirconate titanate (PZT) ceramics, pentavalent donor additions (niobium and tantalum) were reported to produce significant effects on mechanical and electrical properties, characterized by enhanced dielectric constant and dc resistivity and by a well-defined hysteresis loop.[19] This motivated us to study effects of tantalum substitution on the structure, dielectric and piezoelectric properties of $La_2Ti_2O_7$.

2. Experimental Procedure

2.1. *Powder synthesis*

$La_2Ti_{2-x}Ta_xO_7$ ($x = 0, 0.05, 0.1, 0.2$, and 0.3, abbreviated as LTT-0.05, LTT-0.1, LTT-0.2, and LTT-0.3, respectively) powders were prepared by the mixed oxide route using the high-purity raw powders of La_2O_3 (99.99%), Ta_2O_5 (99.85%), and TiO_2 (99.6%). The starting materials were weighted in the appropriate molar ratios according to the formula. The weighed oxides were fully mixed through ball milling for 4 h. The calcination took place in air at 1300°C for 4 h, followed by the second ball milling for 4 h. And the ball milling rotation speed was 350 rpm.

2.2. *Ceramic fabrication*

(A) *Untextured ceramics*: The reground powders were sintered by SPS (HPD 25/1, FCT, Rauenstein, Germany) at 1350°C for 5 min with 50 MPa pressure using a graphite die with 20 mm diameter. The sintered ceramics were annealed at 1000°C for 6 h in an air furnace to remove any carbon contamination, which increased their dc resistivity and density.

(B) *Textured ceramics*: Textured ceramics were prepared using a two-step SPS process. In the first step, the powders were sintered in a graphite die with 20 mm diameter at 1250°C for 3 min under 70 MPa pressure. In the second step, these sintered ceramics were placed in a graphite die of 30 mm diameter and sintered at 1350°C for 5 min with 50 MPa pressure. The compressive stress of 50 MPa was applied within 1 min of reaching 1350°C. Finally, the sintered ceramics were annealed at 1250°C for 10 h in an air furnace to remove carbon contamination.

2.3. *Characterization*

The phase purity of the $La_2Ti_{2-x}Ta_xO_7$ calcined powders was checked using a X-ray diffractometer (Model X'Pert PRO, PANalytical, Almelo, Holland) with $CuK_{\alpha 1}$ (1.54059 Å) radiation over a range of $2\theta = 10$–60°. The degree of grain orientation for textured ceramics was quantified using the Lotgering orientation factor (LOF), $f = (P - P_o)/(1 - P_o)$, where $P = \sum I(h00)/\sum I(hkl)$ from 15–50° of 2θ values; $P_o = P$ for a nonoriented sample. The apparent densities of the sintered and annealed ceramics were measured by Archimedes method. Scanning electron microscopy (SEM, JEOL JSM-5610LV) and Transmission Electron Microscopy (TEM, JEOL 2010) were employed to examine the microstructures of the specimens. Prior to dielectric and ferroelectric measurements, platinum paste was painted on opposite faces of the samples to fabricate electrodes, which was dried, decomposed and hardened by gradually heating to 900°C. The dielectric properties were characterized in the frequency range of 10^2–10^6 Hz with temperature range from 25°C to 1500°C using an HP4284A LCR meter equipped with a tube furnace. The piezoelectric constant d_{33} was measured using a quasi-static d_{33} meter (CAS, ZJ-3B, Institute of Acoustics Chinese Academy of Sciences, Beijing, China) after poling the samples in silicone oil at 200°C under various dc electric fields (10–25 kV/mm). The dc resistivity was measured as a function of temperature using an electrometer (Keithley, Model 6517A, Cleveland, OH, USA) in a high-temperature furnace.

3. Results and Discussion

3.1. *Phase analysis and the dielectric properties of untextured $La_2Ti_{2-x}Ta_xO_7$ ceramics*

Figure 1 shows the XRD patterns of $La_2Ti_{2-x}Ta_xO_7$ powders calcined at 1300°C where $x = 0.05, 0.1, 0.2, 0.3$. The consecutive graphs are displaced vertically for clarity. Within the detection limit of powder XRD, when $x \leq 0.2$ all the observed peaks could be indexed according to the monoclinic structure of $La_2Ti_2O_7$ with $P2_1$ symmetry (JCPDS No. 28-0517). This suggests that single-phase solid solutions were formed with a small amount of tantalum substitution ($x \leq 0.2$). Nevertheless, second phase identified as $La_3Ti_2TaO_{11}$ (JCPDS

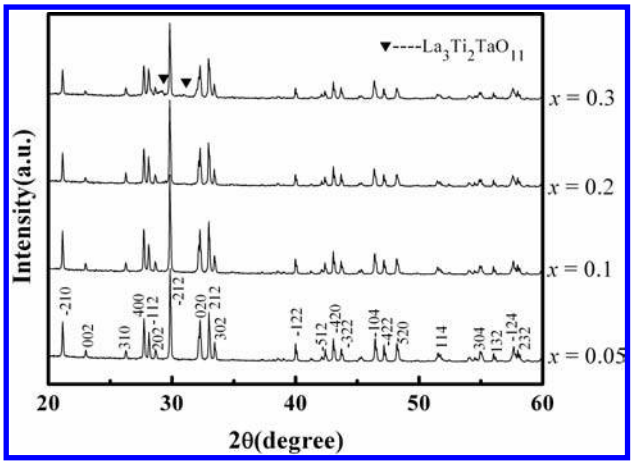

Fig. 1. XRD patterns of $La_2Ti_{2-x}Ta_xO_7$ ($x = 0, 0.05, 0.1, 0.2, 0.3$) powders calcined at 1300°C (black triangles denote reflections from second phase indexed as $La_3Ti_2TaO_{11}$).

No. 54-0632) could be detected when $x = 0.3$, indicating that the solid solution limit of tantalum in $La_2Ti_2O_7$ lattice is in the proximity of $x = 0.2$.

The change in the structure with tantalum substitution might be correlated with the influence of oxygen content. It is accepted that in $A_nB_nO_{3n+2}$ homologous series (also represented by ABO_x, where X denotes oxygen content, $X = 3 + 2/n$) the crystal structure type is related to n value and can be tuned by adjusting oxygen content X.[14] We can figure out that with increase in X value, oxygen content increases, while n value decreases along with the layer thickness in perovskite slabs. In the present case, Ta^{5+} cations that substitute the Ti^{4+} cations clearly act as donors. It is reasonable to propose that the excess of the oxygen contained in Ta_2O_5 could be fully or partially retained, which resulted in increasing oxygen content in $La_2Ti_2O_7$. Thus, the stability of 4-layer perovskite-slabs was reduced and it gradually collapsed into 3-layer structure.

The lattice parameters of $La_2Ti_2O_7$ with tantalum substitution were refined based on the powder X-ray diffractions, shown in Table 1 as a function of tantalum content. It is observed that both a- and b-dimensions increased slightly with increasing Ta^{5+} content, whereas c-dimension exhibited an obvious decrease, which resulted in a slight increase in the unit cell volume. The variation in lattice parameters can be partly explained by the larger ionic radius of Ta^{5+} (0.65 Å) than that of the substituted Ti^{4+} (0.604 Å), which induces an expansion of the crystal structure. These results can be associated to the effect of the tantalum doping on the rotation of the oxygen octahedra. It was reported that the phase transition in $La_2Ti_2O_7$ from orthorhombic $Cmc2_1$ to monoclinic $P2_1$ is achieved by displacement of the La atoms and rotations of the TiO_6 octahedra around the axes parallel to the b crystallographic axis by approximately 10° from the orientation in the $Cmc2_1$ modifications.[20] The incorporation of the tantalum atoms into Ti-sites in $La_2Ti_2O_7$ might induce a decrease in the rotation angle of the oxygen octahedra due to the difference in the ionic radius and valence state. As a consequence, a-dimension was lengthened whereas c-dimension was shortened.

As shown in Table 1, both the theoretical densities and the measured densities of $La_2Ti_{2-x}Ta_xO_7$ ceramics increased with increasing tantalum content, while the relative densities showed a decline. The increase in theoretical density is mainly attributed to the increased molar mass because tantalum atoms (180.95 g/cm^3) are much heavier compared to titanium atoms (47.88 g/cm^3), in spite of the slightly increased unit cell volume. SEM images of fracture surfaces of as-sintered samples were shown in Fig. 2 (with insets showing the thermal-etched surfaces). Significant change in grain size and shape was observed. With increasing Ta content, the grain shape became more spherical and the grain size decreased from 10 to 15 μm for $x = 0.05$ to 1–3 μm for $x = 0.3$. This could be explained by the B-site cation vacancies induced by Ta_2O_5 doping, which tended to aggregate along the grain boundaries. As a result, the grain growth was inhibited, resulting in relatively small grains. Similar phenomenon has been observed in $BaTiO_3$ and $(Na_{1/2}Bi_{1/2})TiO_3$ system.[21–23] Furthermore, the pores of the specimens increased as the doping content increased. The variation of the microstructure coincided with the change in relative densities of the specimens.

Figure 3 shows TEM images of the untextured LTT-0.2 ceramic. A typical grain of LTT-0.2 with size about 1–2 μm was observed in Fig. 3(a), consistent with the SEM results. The high-resolution transmission electron microscopy (HRTEM) was given shown in Fig. 3(c). The d-spacing of the first and the majority plane shown in Fig. 3(c) were ~12 Å, corresponding to the 4-layer $La_2Ti_2O_7$. However, a planar defect was clearly seen in Fig. 3(b), which might be related to the donor doping effect of tantalum.

The frequency dependence of room temperature dielectric constant (ε_r) and loss tangent (tan δ) of Ta-doped $La_2Ti_2O_7$ specimens is shown in Fig. 4. For each composition, the dielectric constant exhibited a slight dependence on frequency. At 1 kHz, ε_r of LTT-0.05 was ~49.2; with increasing Ta content, the dielectric constant showed an obvious decrease to 43.3 for LTT-0.2, while it was increased to 46.0 for LTT-0.3. The decrease in dielectric constant might be related to the reduced intrinsic dielectric polarization by tantalum substitution. The loss tangent exhibited relatively weak compositional dependence and an obvious decrease with increasing frequency was observed. The tan δ values for all compositions were in the order of 10^{-4} at 1 kHz.

Figure 5 shows the temperature dependence of dielectric constant and loss tangent at various frequencies measured on the untextured $La_2Ti_{2-x}Ta_xO_7$ ceramics. For LTT-0.05 and LTT-0.2, a step-like dielectric constant anomaly accompanied by a peak in the corresponding curve of tan $\delta - T$ was observed at the measured frequencies and it was ascribed to be

Table 1. The lattice parameters of Ta-doped $La_2Ti_2O_7$ powders and the densities of untextured ceramics.

			Crystal parameters				
x	Calculated density (g/cm^3)	Measured density (g/cm^3)	a (Å)	b (Å)	c (Å)	γ (°)	V (Å^3)
0.05	5.862	5.796	7.8181	13.0121	5.5457	98.607	557.81
0.1	5.938	5.827	7.8220	13.0122	5.5451	98.587	558.06
0.2	6.091	5.952	7.8291	13.0145	5.5447	98.611	558.59
0.3	6.249	6.053	7.8284	13.0153	5.5448	98.607	558.59

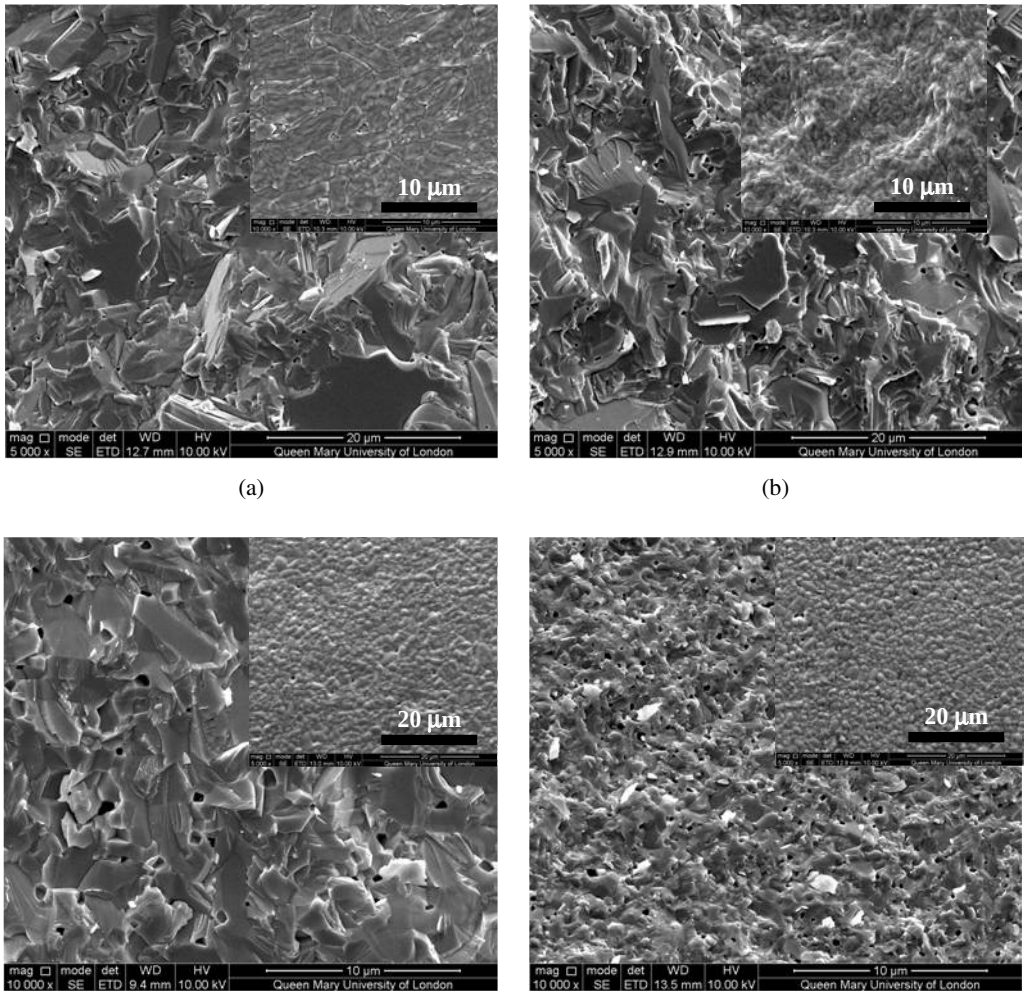

Fig. 2. SEM images of fracture surfaces as-sintered $La_2Ti_{2-x}Ta_xO_7$ ceramics (with insets showing the thermal-etched surfaces): (a) $x = 0.05$, (b) $x = 0.1$, (c) $x = 0.2$, and (d) $x = 0.3$.

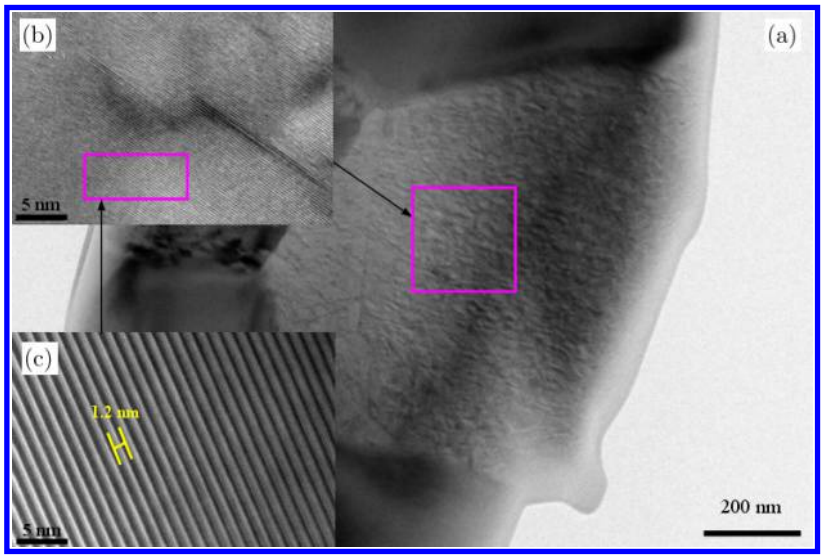

Fig. 3. (a) TEM images from the untextured LTT-0.2 ceramic, (b) an enlarged area from, and (c) high resolution image of a selected area.

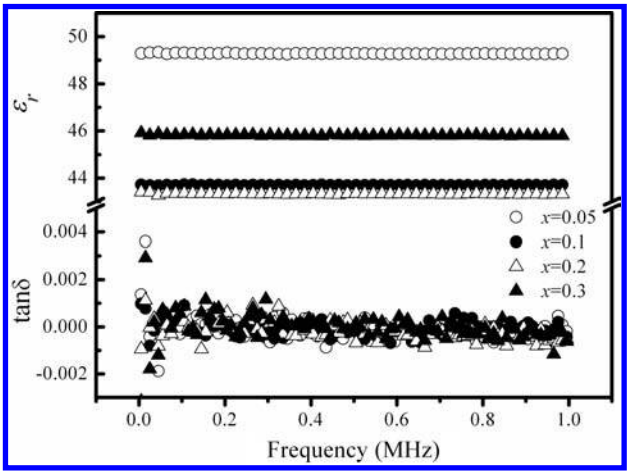

Fig. 4. The frequency dependence of dielectric constant and loss tangent of Ta-doped $La_2Ti_2O_7$ specimens.

the phase transition from orthorhombic $Cmc2_1$ to $Cmcm$. However, for LTT-0.1, only the step-like dielectric constant anomaly appeared and no dielectric anomaly was detected for LTT-0.3 owing to the high losses at high temperatures. The Curie points obtained from the dielectric constant peaks for LTT-0.05, LTT-0.1, and LTT-0.2 were about $1410 \pm 5°C$, $1393 \pm 5°C$, and $1396 \pm 5°C$, respectively. Compared to the T_c of pure $La_2Ti_2O_7$ ($T_c \sim 1461 \pm 5°C$),[12] it is easily seen that with increasing Ta content, T_c decreases markedly. The variation of T_c has been found to strongly correlate with the structural distortion.[24,25] In $La_2Ti_2O_7$, the phase transition from $Cmc2_1$ to $Cmcm$ at 1460°C involves the rotations of oxygen octahedra along a crystallographic directions, accompanied by a reduction in the distortion of oxygen octahedra.[20] Therefore, it is concluded that the decrease in the Curie points of Ta-doped $La_2Ti_2O_7$ can be related to the incorporation of tantalum into $La_2Ti_2O_7$ lattice which assisted the rotations and reduced the distortions of oxygen octahedra. This result is in agreement with the variation in lattice parameters. Furthermore, we observed that the variation in Curie temperature with increasing tantalum content vanished at $x = 0.2$. This further confirmed the solution limit of tantalum in $La_2Ti_2O_7$, which is consistent with the XRD results.

A careful examination reveals an additional dielectric anomaly in the low temperature region, as shown in the insets of Figs. 5(a) and 5(b). A similar dielectric anomaly was previously reported in Ce-substituted $La_2Ti_2O_7$ systems[18] in the same temperature region and it was ascribed to be related

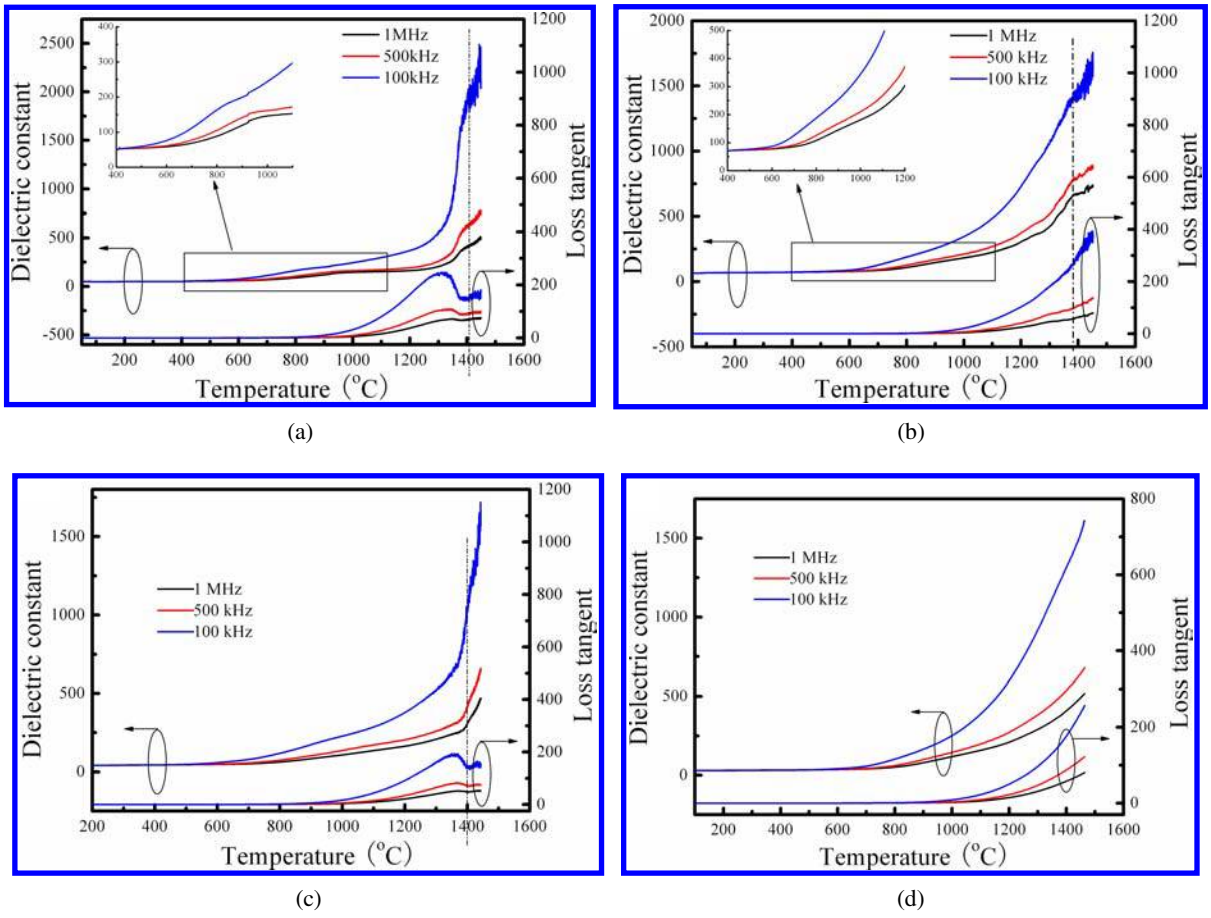

Fig. 5. The temperature dependence of dielectric constant and loss tangent of Ta-doped $La_2Ti_2O_7$ specimens: (a) $x = 0.05$, (b) $x = 0.1$, (c) $x = 0.2$, and (d) $x = 0.3$.

with point effect in the materials. However, considering that the phase transition from *Cmcm* to $Cmc2_1$ during cooling occurred in the vicinity of 780°C, further studies are needed to clarify this low-temperature dielectric anomaly.

Ta^{5+} incorporating into Ti^{4+} sites as a donor produces an extra positive charge. Because of the constraint of the electrical charge neutrality in the compound, substitution of pentavalent Ta^{5+} for tetravalent Ti^{4+} should accompany either electrons or cation vacancies from ionic considerations. The corresponding compensation mechanisms are: (1) electronic compensation (compensated by electrons, Eq. (1)) and (2) ionic compensation (compensated by cation vacancies, Eq. (2)), which can be expressed as follow:

$$Ta_2O_5 \xrightarrow{2(TiO_2)} 2Ta_{Ti}^{\bullet} + 4O_O + e' + 1/2O_2, \quad (1)$$

$$2Ta_2O_5 \xrightarrow{4(TiO_2)} 4Ta_{Ti}^{\bullet} + 10O_O + V_{Ti}^{4/}. \quad (2)$$

It is clear that for electronic compensation, the excess oxygen contained in Ta_2O_5 oxide is lost. However, the excess oxygen is retained in terms of cations vacancies compensation. Further, we can see that different compensation mechanisms give rise to different electrical behaviors. For ionic compensation, the compensated B-site vacancies are restricted in the lattice and it is difficult for them to move; thus, they have no contribution to conductivity. However, if the dominating compensation species are electrons, the electrical conductivity can be enhanced due to the electron mobility; and this can result in deterioration of the insulation of $La_2Ti_2O_7$ ceramics.

The temperature-dependent dc resistivities (ρ) for all the four samples are shown in Fig. 6. As seen, the dc resistivity exhibits strong dependence on temperature and composition. With increasing temperature, it shows a monotonous decrease, suggesting the thermally activated nature of resistivity. Further, with increasing tantalum doping content, a clear decrease in dc resistivity values was observed followed by an increase in resistivity. At 600°C, the dc resistivity of LTT-0.05 is about $3.4 \times 10^6 \Omega \cdot$ cm, while it was lowered by almost an order to $\sim 3.6 \times 10^5\ \Omega \cdot$ cm for LTT-0.1. In contrast, the resistivity of LTT-0.2 ceramics was much higher ($\rho \sim 1.0 \times 10^8\ \Omega \cdot$ cm). The temperature-dependent resistivity was fitted by the Arrhenius Law. A plot of $\ln \rho$ against

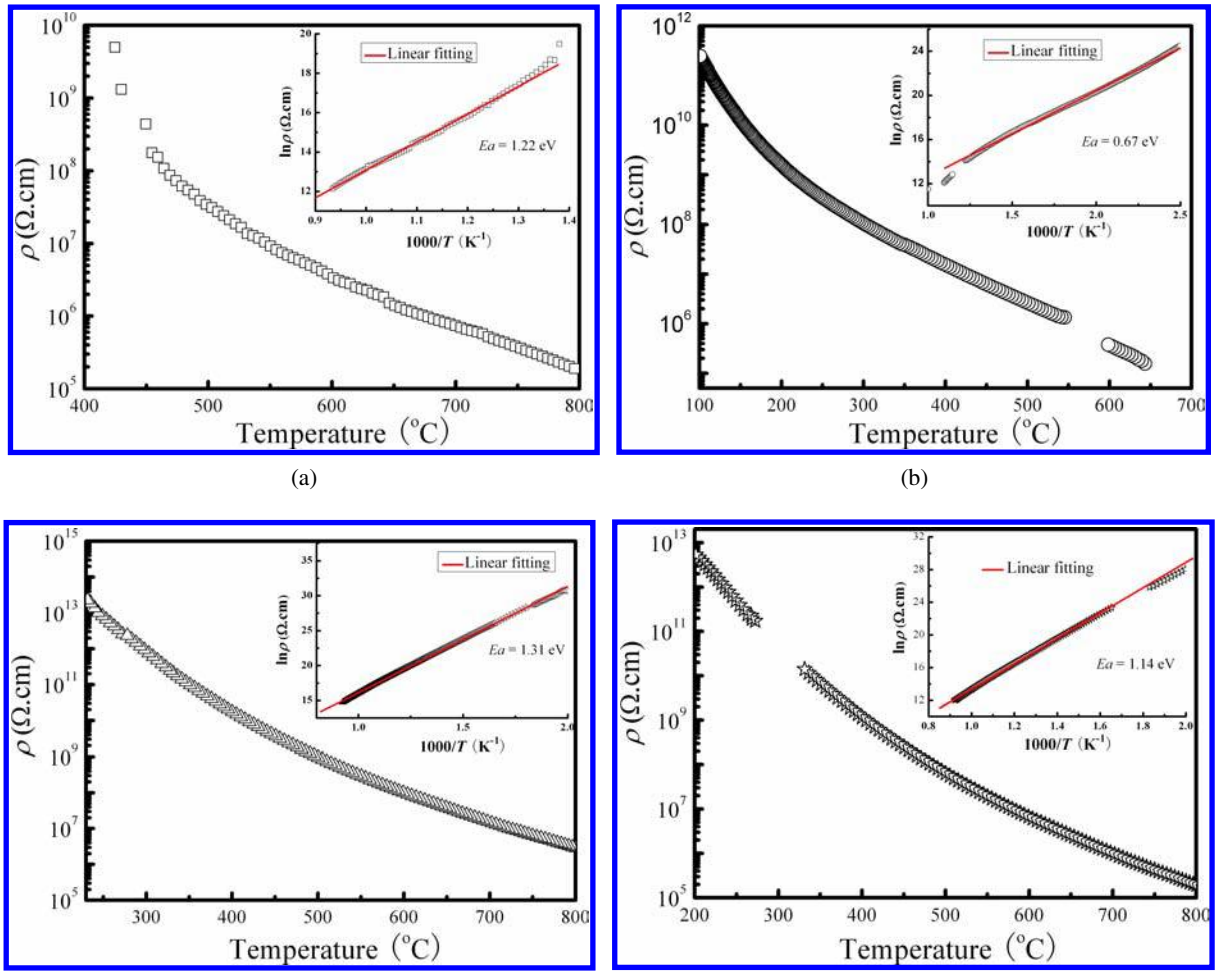

Fig. 6. The temperature-dependent dc resistivities (ρ) for all the four samples: (a) $x = 0.05$, (b) $x = 0.1$, (c) $x = 0.2$, and (d) $x = 0.3$.

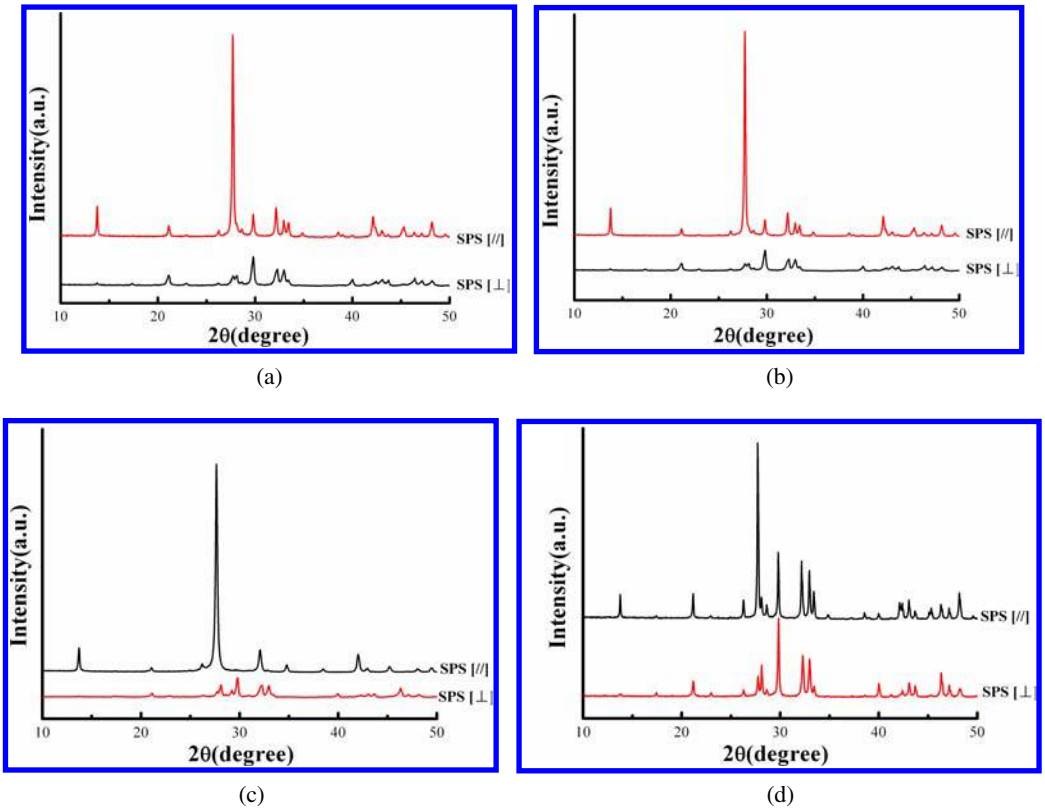

Fig. 7. XRD of textured $La_2Ti_{2-x}Ta_xO_7$ ceramics performed on the planes parallel and perpendicular to the pressing direction: (a) $x = 0.05$, (b) $x = 0.1$, (c) $x = 0.2$, and (d) $x = 0.3$.

reciprocal temperature was given in the insets of Fig. 6. The linear fitting gives activation energies of 1.22, 0.67, 1.31, and 1.14 eV for LTT-0.05, LTT-0.1, LTT-0.2, and LTT-0.3, respectively. It is reported that the activation energy for the mobility of carrier charges is strongly associated with their concentrations.[26] Therefore, it is reasonable to propose that the carrier charge concentration in LTT-0.1 is much higher than others, resulting in the lower resistivity. And the higher resistivity of LTT-0.2 ceramics can be explained by the fact that there are less charge carriers.

These results, together with XRD analysis support that the compensation mechanism is dominated by electrons for composition with lower tantalum doping content ($x \leq 0.1$), whereas beyond this value the dominating mechanism changed to ionic compensation.

3.2. *Effect of grain orientation on the piezoelectric properties of $La_2Ti_{2-x}Ta_xO_7$ ceramics*

For polycrystalline ferroelectric ceramics, the grain orientation is randomly distributed and there may be several ferroelectric domains contained in one grain. Thus, domain switching under electrical poling is constrained by differently oriented neighboring grains, which makes ceramics difficult to be poled with respect to single crystals. It is well accepted that high-textured ceramics with oriented grains exhibit pseudo-single crystal structure[27] and they are easier to be poled because of their lower E_c compared with the untextured ceramics. Therefore, in the present section, SPS was employed to fabricate textured $La_2Ti_{2-x}Ta_xO_7$ ceramics to enhance the piezoelectric activity.

Figure 7 shows room temperature XRD patterns of textured $La_2Ti_{2-x}Ta_xO_7$ ceramics performed on the surface with its normal line parallel to the pressing direction (SPS[//]). Single phase could be obtained for $x = 0.05, 0.1$, and 0.2. All the observed peaks matched JCPDS No. 28-0517 of $La_2Ti_2O_7$ except for the difference in relative intensity because of the grain orientation, which was characterized by some strong (h00) reflections. As shown in Table 2, the LOF, f, was quantified to be 0.724, 0.683, 0.671, and 0.542 for

Table 2. The relative densities, LOHs (f), room temperature dielectric properties (ε_r and tan δ), and piezoelectric coefficients (d_{33}) of textured $La_2Ti_{2-x}TaxO_7$ ceramics.

				ε_r (1 MHz)		tan δ (1 MHz)	
x	ρ (%)	f	d_{33} (pC/N)	SPS[//]	SPS[⊥]	SPS[//]	SPS[⊥]
0.05	98.5	0.724	1.4 ± 0.1	48.6	51.3	0.00017	0.00033
0.1	98.0	0.683	–	44.2	47.5	0.00184	0.00241
0.2	97.4	0.671	2.1 ± 0.1	41.7	45.8	0.00035	0.00048
0.3	96.8	0.542	0.9 ± 0.1	43.9	48.1	0.00051	0.00092

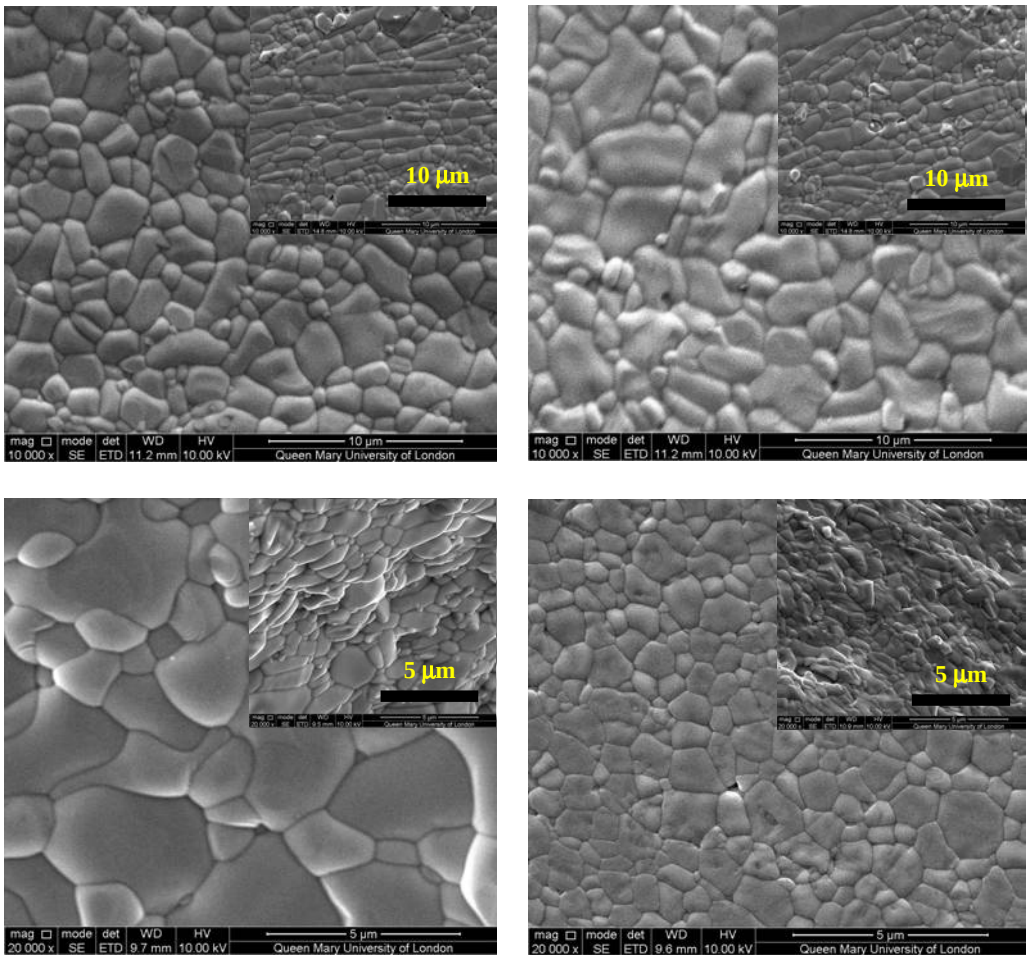

Fig. 8. SEM images of the parallel surfaces of the textured ceramics (with insets showing the perpendicular surfaces): (a) $x = 0.05$, (b) $x = 0.1$, (c) $x = 0.2$, and (d) $x = 0.3$.

LTT-0.05, LTT-0.1, LTT-0.2, and LTT-0.3, respectively. When sintered at the same conditions, the orientation factor decreased with increasing amount of tantalum. Table 2 also listed the room temperature dielectric properties of textured $La_2Ti_{2-x}Ta_xO_7$ ceramics. Both dielectric constant and loss tangent showed strong anisotropy. Both of them are higher along SPS[⊥] direction than those along SPS [//] direction. This is because SPS[⊥] direction is consistent with the spontaneous polarization direction. Similar results were found in textured $Nd_2Ti_2O_7$ and $Sr_2Nb_2O_7$ ceramics.[12,28]

SEM images performed on the surfaces with their respective normal line perpendicular to (SPS[⊥]) and parallel to the pressing direction (SPS[//]) were shown in Fig. 8. All ceramics except for LTT-0.3 exhibited preference in the grain orientation along directions perpendicular to pressing direction. With increasing tantalum additions, the average grain size decreased and the grain shape became less plate-like. This is evident with the decreasing LOF value, particularly for LTT-0.3.

The piezoelectric constant, d_{33}, measured on a direction perpendicular to the pressing direction (SPS[⊥]), were summarized in Table 2. With increasing amount of tantalum substitution, d_{33} increased slightly, reaching a maximum value of ~2.1 pC/N at $x = 0.2$, which is higher than that of pure $La_2Ti_2O_7$ with similar texture.[12] And then, it dropped with further increasing tantalum content. For LTT-0.1, no d_{33} value was obtained because of the high conductivity and the sample was broken down before the peak driving field was applied. The variation in piezoelectric constant might be associated with tantalum substitution and the effect of texture.

When compared with the commercially used piezoelectric ceramics as accelerometers and vibration sensors,[1] such as α-SiO_2 ($T_c \sim 573°C$, $d_{11} \sim 2$ pC/N), $LiNbO_3$ ($T_c \sim 1150°C$, $d_{33} \sim 6$ pC/N), $Na_{0.5}Bi_{4.5}Ti_4O_{15}$ ($T_c \sim 600°C$, $d_{11} \sim 18$ pC/N), the T_c value of LTT-0.2 was much higher ($T_c \sim 1396 \pm 5°C$) and the d_{33} value was competitive with that of α-SiO_2. These merits make these ceramics potential materials for high-temperature piezoelectric applications. Further progress is focused on improvement of d_{33} value for LTT-0.2 through optimizing the synthesis process to make ceramics with higher grain orientation.

4. Conclusions

Dense polycrystalline ceramics with a general formula, $La_2Ti_{2-x}Ta_xO_7$ ($x = 0.05, 0.1, 0.2$, and 0.3) were prepared by SPS method and the corresponding highly textured ceramics were synthesized through a two-step SPS process. The structure changed gradually from 4-layer to 3-layer due to the increasing oxygen content obtained from the extra oxygen in Ta_2O_5. The ferroelectric Curie point (T_c) decreased with increasing tantalum doping content. Their energy band gaps (E_g) monotonically decreased with tantalum doping, while dc resistivity reached a maximum value of $\sim 1.0 \times 10^8\ \Omega \cdot$ cm at 600°C for $x = 0.2$. The piezoelectric coefficient (d_{33}) of $La_2Ti_{2-x}Ta_xO_7$ increased at first, and then decreased with Ta doping. A maximum value was obtained at $x = 0.1$ with a $d_{33} \sim 2.1$ pC/N. These merits make these ceramics potential materials for high-temperature piezoelectric applications.

Acknowledgments

This work is supported by the National Basic Research Program of China (2009CB623306), International Science & Technology Cooperation Program of China (2013DFR50470). C. C. Li would thank China Scholarship Council for supporting his studies.

References

[1]R. C. Turner, P. A. Fuierer, R. E. Newnham and T. R. Shrout, Materials for high temperature acoustic and vibration sensors: A review, *Appl. Acoust.* **41**, 299 (1994).

[2]D. Damjanovic, Materials for high temperature piezoelectric transducers, *Curr. Opin. Solid State Mater. Sci.* **3**, 469 (1998).

[3]H. Yan, H. Zhang, R. Ubic, M. J. Reece, J. Liu, Z. Shen and Z. Zhang, A lead-free high-curie-point ferroelectric ceramic, $CaBi_2Nb_2O_9$, *Adv. Mater.* **17**, 1261 (2005).

[4]S. J. Zhang, R. Xia, L. Lebrun, D. Anderson and T. R. Shrout, Piezoelectric materials for high power, high temperature applications, *Mater. Lett.* **59**, 3471 (2005).

[5]Q. Zhang, Z. R. Li, F. Li, Z. Xu and X. Yao, Temperature dependence of dielectric/piezoelectric properties of $(1\text{-}x)Bi(Mg_{1/2}Ti_{1/2})O_{3-x}PbTiO_3$ ceramics with an MPB composition, *J. Am. Ceram. Soc.* **93**, 3330 (2010).

[6]Y. Saito, H. Takao, T. Tani, T. Nonoyama, K. Takatori, T. Homma, T. Nagaya and M. Nakamura, Lead-free piezoceramics, *Nature* **432**, 84 (2004).

[7]H. L. Du, W. C. Zhou, F. Luo and D. M. Zhu, Perovskite lithium and bismuth modified potassium-sodium niobium lead-free ceramics for high temperature applications, *Appl. Phys. Lett.* **91**, 182909 (2007).

[8]C. M. Wang, J. F. Wang, S. J. Zhang and T. R. Shrout, Piezoelectric and electromechanical properties of ultrahigh temperature $CaBi_2Nb_2O_9$ ceramics, *Physica Status Solidi A* **3**, 49 (2009).

[9]J. Tellier, Ph. Boullay, M. Manier and D. Mercurio, A comparitive study of the Aurivillius phase ferroelectrics $CaBi_4Ti_4O_{15}$ and $BaBi_4Ti_4O_{15}$, *J. Solid State Chem.* **177**, 1829 (2004).

[10]J. K. Yamamoto and A. S. Bhalla, Piezoelectric properties of layered perovskite $A_2Ti_2O_7$ (A = La and Nd) single-crystal fibers, *J. Appl. Phys.* **70**, 4469 (1991).

[11]S. Nanamatsu, M. Kimura, K. Doi, S. Matsushita and N. Yamada, A new ferroelectric: $La_2Ti_2O_7$, *Ferroelectrics* **8**, 511 (1974).

[12]H. X. Yan, H. P. Ning, Y. M. Kan, P. L. Wang and M. J. Reece, Piezoelectric ceramics with super-high curie points, *J. Am. Ceram. Soc.* **92**, 2270 (2009).

[13]P. A. Fuierer and R. E. Newnham, $La_2Ti_2O_7$ ceramics, *J. Am. Ceram. Soc.* **74**, 2876 (1991).

[14]F. Lichtenberg, A. Herrnberger and K. Wiedenmann, Synthesis, structural, magnetic and transport properties of layered perovskite-related titanates, niobates and tantalates of the type $A_nB_nO_{3n+2}$, $A'A_{k-1}B_kO_{3k+1}$ and $A_mB_{m-1}O_{3m}$, *Prog. Solid State Chem.* **36**, 253 (2008).

[15]S. Nanamatsu, M. Kimura and T. Kawamura, Crystallographic and dielectric properties of ferroelectric $A_2B_2O_7$ (A = Sr, B = Ta, Nb) crystals and solid solutions, *J. Phys. Soc. Jpn.* **38**, 817 (1975).

[16]H. P. Ning, H. X. Yan and M. J. Reece, Piezoelectric strontium niobate and calcium niobate ceramics with super-high curie points, *J. Am. Ceram. Soc.* **93**, 1409 (2010).

[17]M. Kimura, S. Nanamatsu, K. Doi, S. Matsushita and M. Takahashi, Electrooptic and piezoelectric properties of $La_2Ti_2O_7$ single crystal, *Jpn. J. Appl. Phys.* **11**, 904 (1972).

[18]Z. P. Gao, H. X. Yan, H. P. Ning, R. Wilson, X. Y. Wei, B. Shi, H. Ye and M. J. Reece, Piezoelectric and dielectric properties of Ce substituted $La_2Ti_2O_7$ ceramics, *J. Eur. Ceram. Soc.* **33**, 1001 (2013).

[19]R. Gerson, Variation in ferroelectric characteristics of lead zirconate titanate ceramics due to minor chemical modifications, *J. Appl. Phys.* **31**, 188 (1960).

[20]N. Ishizawa, F. Marumo, S. Iwai, M. Kimura and T. Kawamura, Compounds with perovskite-type slabs. V. A high-temperature modification of $La_2Ti_2O_7$, *Acta Crystallogr.* **B38**, 368 (1982).

[21]V. Lewis, R. A. Catlow and R. E. W. Casselton, PTCT effect in $BaTiO_3$, *J. Am. Ceram. Soc.* **68**, 555 (1985).

[22]J. Y. Yi, J. K. Lee and K. S. Hong, Dependence of the microstructure and the electrical properties of lanthanum-substituted $(Na_{1/2}Bi_{1/2})TiO_3$ on cation vacancies, *J. Am. Ceram. Soc.* **85**, 3004 (2002).

[23]Y. S. Sung and M. H. Kim, Effects of B-site donor and acceptor doping in Pb-free $(Bi_{0.5}Na_{0.5})TiO_3$ ceramics, *Ferroelectrics* **13**, 217 (2010).

[24]Y. Shimakawa and Y. Kubo, Crystal and electronic structures of $Bi_{4-x}La_xTi_3O_{12}$ ferroelectric materials, *Appl. Phys. Lett.* **79**, 2791 (2001).

[25]H. Sun and X. B. Chen, Structure and ferroelectric properties of stoichiometric and Sr-deficient–$SrBi_4Ti_4O_{15}$ thin films, *J. Mater. Sci.* **46**, 1581 (2011).

[26]S. Steinsvik, R. Bugge, J. Gjønnes, J. Taftø and T. Norby, The defect structure of $SrTi_{1-x}Fe_xO_{3-y}$ (x = 0-0.8) investigated by electrical conductivity measurements and electron energy loss spectroscopy (EELS), *J. Phys. Chem. Solids* **58**, 969 (1997).

[27]H. Yan, M. J. Reece, J. Liu, Z. Shen, Y. Kan and P. Wang, Effect of texture on dielectric properties and thermal depoling of $Bi_4Ti_3O_{12}$ ferroelectric ceramics, *J. Appl. Phys.* **100**, 076103 (2006).

[28]H. P. Ning, H. X. Yan and M. J. Reece, Piezoelectric strontium niobate and calcium niobate ceramics with super-high curie points, *J. Am. Ceram. Soc.* **93**, 1409 (2010).